EBioMedicine 48 (2019) 49–57

Contents lists available at ScienceDirect

EBioMedicine

journal homepage: www.elsevier.com/locate/ebiom

EBioMedicine
Published by THE LANCET

Metabolomic profiling identifies pathways associated with minimal residual disease in childhood acute lymphoblastic leukaemia

Jeremy M. Schraw[a,b,*], Jacob J. Junco[b,c], Austin L. Brown[b,c], Michael E. Scheurer[a,b,c], Karen R. Rabin[b,c,1], Philip J. Lupo[a,b,c,1]

[a] Department of Medicine, Section of Epidemiology and Population Sciences, Baylor College of Medicine, Houston, TX, USA
[b] Texas Children's Cancer and Hematology Centers, Texas Children's Hospital, Houston TX, USA
[c] Department of Paediatrics, Section of Hematology-Oncology, Baylor College of Medicine, Houston TX, USA

ARTICLE INFO

Article history:
Received 5 August 2019
Revised 29 September 2019
Accepted 30 September 2019
Available online 17 October 2019

Keywords:
Acute lymphoblastic leukaemia
Minimal residual disease
Epidemiology
NAMPT
NAMPT inhibitors

ABSTRACT

Background: End-induction minimal residual disease (MRD) is the strongest predictor of relapse in paediatric acute lymphoblastic leukaemia (ALL), but an understanding of the biological pathways underlying early treatment response remains elusive. We hypothesized that metabolomic profiling of diagnostic bone marrow plasma could provide insights into the underlying biology of early treatment response and inform treatment strategies for high-risk patients.

Methods: We performed global metabolomic profiling of samples from discovery ($N = 93$) and replication ($N = 62$) cohorts treated at Texas Children's Hospital. Next, we tested the cytotoxicity of drugs targeting central carbon metabolism in cell lines and patient-derived xenograft (PDX) cells.

Findings: Metabolite set enrichment analysis identified altered central carbon and amino acid metabolism in MRD-positive patients from both cohorts at a 5% false discovery rate. Metabolites from these pathways were used as inputs for unsupervised hierarchical clustering. Two distinct clusters were identified, which were independently associated with MRD after adjustment for immunophenotype, cytogenetics, and NCI risk group. Three nicotinamide phosphoribosyltransferase (NAMPT) inhibitors, which reduce glycolytic/TCA cycle activities, demonstrated nanomolar-range cytotoxicity in B- and T-ALL cell lines and PDX cells.

Interpretation: This study provides new insights into the role of central carbon metabolism in early treatment response and as a potential targetable pathway in high-risk disease.

Funding: American Society of Hematology; Baylor College of Medicine Department of Paediatrics; Cancer Prevention and Research Institute of Texas; the Lynch family; St. Baldrick's Foundation with support from the Micaela's Army Foundation; United States National Institutes of Health.

Research in context

Evidence before this study

End-induction minimal residual disease is the strongest risk factor for relapse in childhood acute lymphoblastic leukemia (ALL). Attempts to improve outcomes in minimal residual disease-positive ALL patients by intensifying conventional chemotherapy have recently resulted in unacceptable toxicities. There is therefore a need for novel, targeted therapeutic agents to drive continued improvements in ALL cure rates. Efforts to develop and test such therapies are limited by a paucity of knowledge concerning mechanisms of chemoresistance. Since metabolomics is acknowledged to be the '-omics' discipline most proximal to the phenotype, and may change rapidly in response to disease state and treatment status, we reviewed the metabolomics literature for studies of ALL patients. We found that this approach had not been leveraged to elucidate mechanisms of chemoresistance, or identify high-risk patients.

Added value of this study

Using a two-stage discovery and replication approach, we identified an association between central carbon metabolism and min-

* Corresponding author at: 1 Baylor Plaza MS: BCM307, Houston TX 77030, USA.
E-mail address: schraw@bcm.edu (J.M. Schraw).
[1] These authors contributed equally to this work.

https://doi.org/10.1016/j.ebiom.2019.09.033

imal residual disease which was independent of National Cancer Institute risk group, immunophenotype, and cytogenetics in $N = 155$ patients treated on or according to Children's Oncology Group protocols. Through subsequent drug sensitivity screens we demonstrated that agents targeting this pathway demonstrate anti-leukemic effects in ALL cell lines and mice bearing patient-derived xenografts. These findings highlight the potential utility of metabolomic screening for risk stratification and assignment of targeted therapies.

Implications of all the available evidence

Our global metabolomic screening approach identified a patient cluster characterized by differential central carbon metabolism, who were at high risk of minimal residual disease. Agents targeting this metabolic pathway demonstrated anti-leukemic effects at dose ranges that have previously been shown to be achievable and well-tolerated in patients with advanced solid tumors. These findings suggest that metabolomic screening has added value for identifying high risk ALL patients and assigning targeted therapies.

1. Introduction

The past several decades have witnessed dramatic improvement in survival for paediatric patients with acute lymphoblastic leukaemia (ALL), due to the advent of risk-stratified chemotherapy, the use of minimal residual disease (MRD) to identify patients in need of more intensified therapy, and the discovery of new molecular subtypes, some with targetable driver mutations [1–3]. The combination of established clinical risk factors, MRD, and next-generation genomic testing has improved risk-directed treatment and outcomes in childhood ALL [4–7]. End-induction MRD response remains the most powerful predictor of relapse [[8],[9]]. The primary strategy to prevent relapse in MRD-positive ALL has historically been to intensify conventional chemotherapy, which initially improved outcomes [10–12] but more recently has led to unacceptable toxicity [13–15]. Thus, novel approaches are essential to bring about further improvements in outcome for chemoresistant disease. Such approaches will depend on novel insights into the underlying biology of chemotherapy resistance.

Metabolomics, the systematic identification of the metabolic products of a biological system, holds promise as a way to monitor cancer metabolism and treatment response [16]. Metabolomics has been applied to ALL to describe the bone marrow microenvironment [17], identify diagnostic biomarkers [[18],[19]], study cellular response to anti-leukemic agents [[20],[21]], and identify patients at risk of complications [22]. However, previous studies have not systematically investigated if metabolomics can be used for understanding early treatment response or informing targeted therapeutic approaches. Therefore, the objectives of this study were to determine whether global metabolomic profiling of diagnostic bone marrow plasma from ALL patients could: 1) identify metabolic alterations associated with early treatment response as measured by end-induction MRD positivity or 2) reveal druggable metabolic alterations.

2. Materials and methods

2.1. Patients

We retrospectively identified 60 MRD-positive and 95 MRD-negative patients (total $N = 155$) for whom cryopreserved diagnostic bone marrow plasma was available, who were then randomly divided into discovery ($N = 93$, 60%) and replication ($N = 62$, 40%) cohorts. Males, females, and individuals of all racial/ethnic groups were eligible. All patients were ≤18 years of age at diagnosis. Patients were treated at Texas Children's Hospital from 2007–2018, enrolled on or treated according to Children's Oncology Group (COG) frontline ALL trials as indicated for their disease type and National Cancer Institute (NCI) risk group. Clinical and demographic information, including immunophenotype, cytogenetics, presenting white blood cell (WBC) count, age, sex, height, weight, and race/ethnicity were abstracted from the medical record. The primary study outcome was MRD positivity at day 29 of therapy, defined as ≥0.01% leukemic blasts detected in bone marrow at the end of induction chemotherapy by flow cytometry. Patient samples for in vitro cytotoxicity assays were obtained at the time of ALL diagnosis or relapse from 7 additional paediatric patients treated at Texas Children's Hospital during the same time period. This study was performed in accordance with the Declaration of Helsinki, approved by the Baylor College of Medicine Institutional Review Board and Animal Care and Use Committee, and conforms to the Strengthening the Reporting of Observational Studies in Epidemiology (STROBE) reporting guidelines. Written informed consent was obtained for all study subjects, and assent was obtained where appropriate.

2.2. Metabolomic profiling

Diagnostic bone marrow aspirates were obtained during standard-of-care procedures and centrifuged to harvest plasma, which was then cryopreserved. Global metabolomic profiling was performed by Metabolon (Morrisville, NC). Data were extracted and processed using described methods [23]. Briefly, a pooled matrix sample was generated by taking a small volume of each experimental sample which served as a technical replicate throughout. Instrument variability was determined by calculating the median relative standard deviation (RSD) for the standards that were added to each sample prior to injection into the mass spectrometers. Overall process variability was determined by calculating the median RSD for all endogenous metabolites (i.e., non-instrument standards) present in 100% of the pooled matrix samples. All methods utilized a Waters ACQUITY ultra-performance liquid chromatography (UPLC) and a Thermo Scientific Q-Exactive high resolution/accurate mass spectrometer interfaced with a heated electrospray ionization (HESI-II) source and Orbitrap mass analyser operated at 35,000 mass resolution.

2.3. Statistical analysis

After identification and normalization, metabolite abundances were rescaled such that the median was one, and missing values were imputed with the minimum value observed for the index metabolite. All further analyses were performed using the scaled, imputed data and excluded 'currency' metabolites ubiquitously represented in metabolic pathways [24] as well as metabolites not detected in multiple samples. We tested both individual metabolites and metabolic pathways for associations with MRD. To identify metabolites associated with MRD, we performed Kruskal-Wallis tests comparing metabolite abundance by MRD status. We retained metabolites associated with MRD at $p < 0{\cdot}001$ in the discovery cohort as candidates and repeated testing in the replication cohort, as simulations demonstrated that $p < 0{\cdot}001$ was the most stringent multiple testing correction we could impose in the discovery partition while retaining >80% power to detect a 2-fold change in metabolite abundance. Candidate metabolites associated with MRD at $p < 0{\cdot}05$ in this cohort were considered to have replicated.

We next performed metabolite set enrichment analysis (MSEA) using the Integrated Molecular Pathway Level Analysis Tool (IMPaLA) to identify pathways enriched for differentially abundant

metabolites in MRD-positive patients, separately in the discovery and replication cohorts. Both the Kyoto Encyclopaedia of Genes and Genomes (KEGG) Pathway Database and Metabolon-provided annotations were used to map metabolites to pathways. The Benjamini-Hochberg procedure was used to compute false discovery rate-adjusted p-values (q-statistic) for MSEA, and statistical significance was defined as q-values $\leq$0.05 in both cohorts. Unsupervised hierarchical clustering using Euclidean distance and Ward's method was performed in the R statistical environment (v3•6•0, R Foundation, Vienna, Austria) based on the abundances of metabolites annotating to MRD-associated pathways from MSEA in the combined sample of $N = 155$ children. Logistic regression models were computed to determine the odds ratio (OR) and 95% confidence interval (CI) for MRD positivity according to membership in the resulting clusters, with adjustment for immunophenotype, cytogenetics, and NCI risk group. Children with *BCR-ABL1* fusion, *KMT2A* rearrangement, hypodiploidy (defined as <44 chromosomes), or intrachromosomal amplification of chromosome 21 were considered to have unfavourable cytogenetics and were compared to the reference group of all other children. We assessed whether the addition of metabolomic data to clinical risk factors improved the performance of statistical models for MRD using DeLong's test for correlated receiver operating characteristics curves. Finally, we performed exploratory analyses to determine whether the identified metabolomic profiles were also associated with early relapse (defined as relapse within 3 years of date of diagnosis).

2.4. Cytotoxicity assays

ALL cell lines were obtained from ATCC (Reh, JM1, RS4; 11, NALM6, SUP-B15, CCRF-CEM, Jurkat, HSB-2) and DSMZ (KOPN8, TANOUE) and maintained in culture medium per recommendations. All cells were verified to be mycoplasma-free before initiating experiments. To generate patient-derived xenografts, primary diagnostic ALL patient bone marrow samples (Table S1) were cryopreserved, and later thawed and injected via tail vein into NOD scid gamma (NSG) mice (Jackson Laboratories, Sacramento, CA). Resulting leukemic blasts were later incubated in culture medium for 3 h before plating for cytotoxicity assays. ALL cell lines or patient samples were incubated with the following agents for 48–96 h: FK866, STF 118804, doxorubicin, metformin (Tocris, Minneapolis, MN); GPP 78 (Cayman Chemical, Ann Arbor, MI); doxorubicin and etoposide (Sigma, St. Louis, MO). Vehicle was DMSO 0•05% for all agents except GPP 78 (0•05% methanol) and metformin (1% water). For NAD+ pre-treatment, cells were first incubated for 1 h with vehicle (0•2% water) or 100 µM NAD+ (Cayman Chemical) for 1 h. Following treatment, cells were incubated with Annexin V-APC (Becton Dickinson, Franklin Lakes, NJ) and propidium iodide (PI) (eBioscience, San Diego, CA) and analysed on an LSRII flow cytometer and FlowJo software (Becton Dickinson). ALL patient samples were analysed by ATP assay (Promega, Madison, WI) with luminescence read by a Luminoskan Ascent Microplate Luminometer (Thermo, Waltham, MA).

2.5. Data sharing

Study data have been accessioned into Mendeley Data (DOI: 10.17632/br223h8sdd.1).

2.6. Role of the funding source

The funding agencies had no role in the design, performance, or analysis of the study, nor on the decision to publish.

3. Results

3.1. Central carbon and amino acid metabolism are associated with end-induction MRD

Table 1 lists clinical and demographic characteristics of ALL patients, stratified by cohort. Overall, participants were 60% male, 62% Hispanic, 29% non-Hispanic white, 9% other non-Hispanic, and had a median age of 6•3 years at diagnosis. Sixty MRD-positive cases were identified ($N = 37$ in discovery, $N = 23$ in replication). NCI risk group was associated with MRD in the discovery cohort, whereas T-lineage disease and male sex were associated with MRD in the replication cohort. We identified 18 metabolites associated with MRD at $p < 0•001$ in the discovery cohort (Fig. 1 and Table S2). Three of the 18 metabolites (malate, fumarate, and 2-keto-3-deoxy-gluconate) were independently associated with MRD at $p < 0•05$ in the replication cohort (Table S2). Similar results were obtained when analysis was restricted to B-ALL patients (Table S3). MSEA identified three metabolic pathways associated with MRD at $q \leq 0.05$ in both the discovery and replication cohorts (Table S4): protein digestion and absorption, aminoacyl-tRNA biosynthesis, and central carbon metabolism in cancer.

Unsupervised hierarchical clustering was performed based on abundances of all metabolites which were detected in samples from both cohorts and annotated to MRD-associated pathways identified by MSEA ($N = 39$). Two distinct clusters were identified (Fig. 2), and principal components analysis confirmed that glycolytic, TCA cycle, and amino acid metabolites most strongly influenced cluster membership (Figure S1). The frequency of MRD positivity was 27•8% in Cluster One and 56•9% in Cluster Two (Table 2). Sex, race/ethnicity, body mass index (BMI) category, NCI risk group, immunophenotype, and the proportion of children with unfavourable cytogenetics were not different between clusters. Relative to children in Cluster One, the odds ratio of MRD was increased for children in Cluster Two (OR 3•13, 95% CI 1•54–6•35) after adjustment for immunophenotype, cytogenetics, and NCI risk group. When analyses were stratified by immunophenotype, the aOR of MRD for patients in Cluster Two was 3.09 (95% CI 1.49–6.53) among children with B-ALL. The crude OR of MRD among T-ALL patients in Cluster Two was 6.0, although statistical significance was not reached due to the small number of T-ALL patients ($N = 13$). A significant increase in area under the curve (AUC) for predicting MRD status was observed for the model incorporating both clinical and metabolomic factors relative to the clinical model alone (Fig. 3; $p = 0•02$). Figure S2 presents relative abundances for all metabolites identified in both the discovery and replication cohorts ($N = 557$) for children in each cluster.

Although incomplete follow-up (i.e., not all patients had completed therapy) restricted our ability to fully evaluate relapse in this study, we performed exploratory analyses to determine whether cluster membership was associated with early relapse (defined as less than 3 years from date of diagnosis). We computed logistic regression models to determine the OR of early relapse, adjusting for NCI risk group, immunophenotype, cytogenetics, and end-induction MRD status (positive vs. negative) and found no significant difference (OR 0•59, 95% CI 0•24–1•39 comparing Cluster Two to Cluster One). Results were unchanged when MRD status was removed from the model (OR 0.89, 95% CI 0.39–1.94). However, a larger sample size and longer follow-up would be needed to more fully evaluate relapse.

3.2. NAMPT inhibitors affect central carbon metabolism and demonstrate cytotoxicity

As central carbon metabolism was associated with MRD, we tested the cytotoxicity of agents targeting these pathways (gly-

Table 1
Clinical and demographic characteristics of the study sample by cohort.

	Discovery partition			Replication partition		
	MRD <0.01% (*N* = 56)	MRD ≥0.01% (*N* = 37)	*p*[a]	MRD <0.01% (*N* = 39)	MRD ≥0.01% (*N* = 23)	*p*[a]
Sex, *N*(%)			0.57			0.05
Male	33 (58.9)	24 (64.9)		19 (48.7)	17 (73.9)	
Female	23 (41.1)	13 (35.1)		20 (51.3)	6 (26.1)	
Age [years], median (IQR)	5.3 (5.6)	8.7 (8.7)	0.08	6.4 (9.4)	5.8 (6.7)	0.25
Race-ethnicity, *N*(%)			0.17			0.18
NHW	19 (33.9)	7 (18.9)		14 (35.9)	5 (21.7)	
Hispanic	30 (53.6)	27 (73.0)		24 (61.5)	15 (65.2)	
Other non-Hispanic	7 (12.5)	3 (8.1)		1 (2.6)	3 (13.0)	
BMI category[b], *N*(%)			0.19			0.76
Normal weight	44 (81.5)	25 (69.4)		27 (71.1)	14 (63.6)	
Overweight or obese	10 (18.5)	11 (30.6)		11 (28.9)	8 (36.4)	
NCI risk status[c], *N*(%)			<0.001			0.84
Standard risk	41 (73.2)	13 (35.1)		21 (53.8)	13 (56.5)	
High risk	15 (26.8)	24 (64.9)		18 (46.2)	10 (43.5)	
Immunophenotype, N (%)			0.31			0.03
B-lineage	52 (92.9)	32 (86.5)		39 (100.0)	19 (82.6)	
T-lineage	4 (7.1)	5 (13.5)		0 (0.0)	4 (17.4)	
Cytogenetics[d], *N*(%)			0.08			0.45
Favorable or neutral	51 (91.1)	29 (78.4)		33 (84.6)	21 (91.3)	
Unfavorable	5 (8.9)	8 (21.6)		6 (15.4)	2 (8.7)	

Abbreviations. MRD, minimal residual disease; NHW, non-Hispanic white; BMI, body mass index.
[a] All *p*-values for categorical values from χ^2 test. *p*-value for age at diagnosis from Kruskal-Wallis test.
[b] Overweight defined as age- and sex-adjusted BMI ≥ 85th percentile. Obese defined as age- and sex-adjusted BMI ≥95th percentile. Not computed for children <2 years of age.
[c] High risk defined as presenting white blood cell count >50,000 cells/μL and/or age at diagnosis ≥10 years.
[d] Unfavorable cytogenetics defined as presence of *BCR-ABL1, KMT2A* rearrangement, hypodiploidy (<44 chromosomes), or iAMP21 at diagnosis.

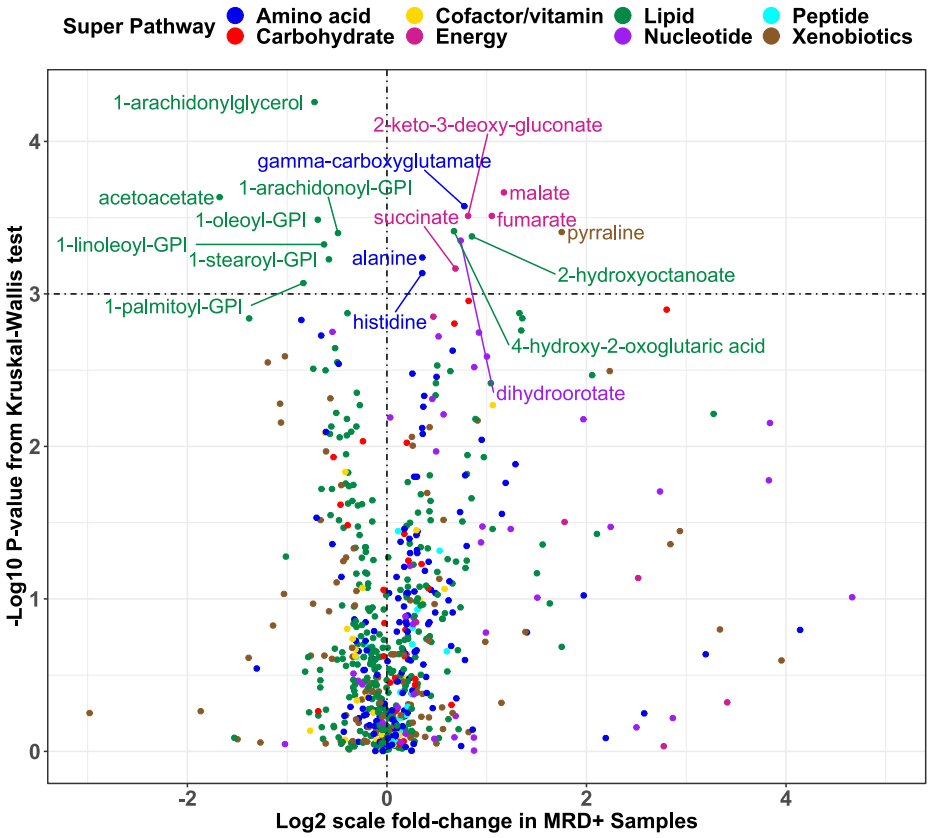

Fig. 1. Univariate associations between metabolite abundances and end-induction MRD. X-axis shows log2-scale mean fold-change in MRD-positive compared to MRD-negative children in the discovery partition while y-axis indicates statistical significance. The dashed vertical line corresponds to no difference in mean abundance by MRD status. The dashed horizontal line represent the pre-defined threshold for statistical significance in the discovery partition of $p < 0.001$.

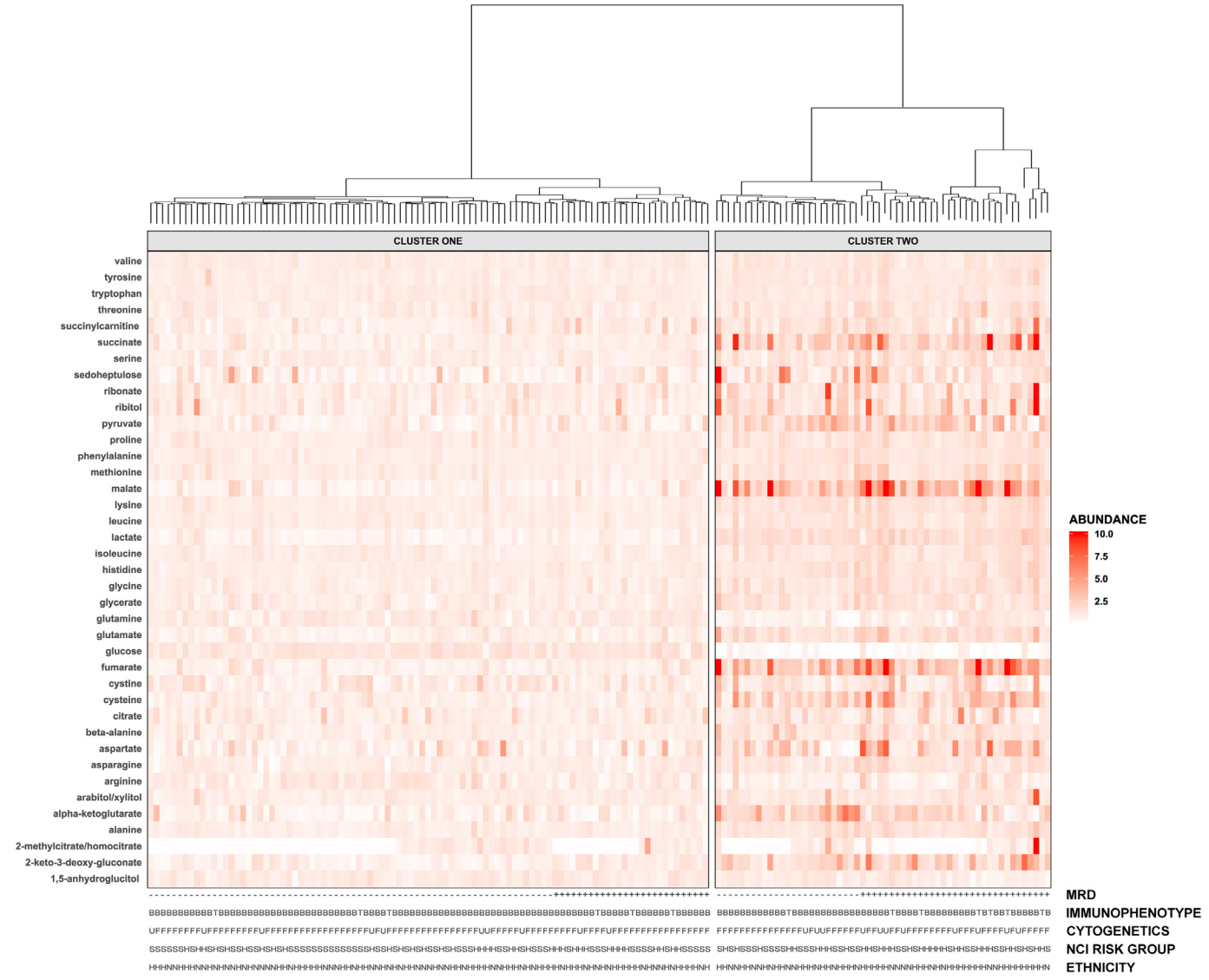

Fig. 2. Hierarchical clustering based on MRD-associated metabolites and pathways in the combined discovery and replication cohorts identifies two groups of patients with differential rates of MRD positivity. Patients shown in columns and metabolites in rows. Top: horizontal grey bars and cluster dendrogram indicating cluster membership. Right: Shading indicates metabolite abundance in each sample relative to the overall mean; darker colors represent greater relative abundance. Extreme values (>10-fold increase) are suppressed for visualization purposes. Bottom: patient's MRD status, immunophenotype (B: B-lineage; T: T-lineage), cytogenetic findings (F: favourable/neutral; U: unfavourable), NCI risk group (S: standard risk; H: high risk), and ethnicity (H: Hispanic; N: Non-Hispanic).

colysis, TCA cycle, and pentose phosphate pathway). Nicotinamide phosphoribosyltransferase (NAMPT) is a key enzyme involved in NAD+ generation, which is critical for glycolysis. It has been shown that NAMPT inhibition also reduces TCA cycle flux in multiple myeloma cells [25], and results in depletion of malate/fumarate in ovarian cancer cells, colorectal cancer cells, and primary myotubes [26–28]. Because malate and fumarate were independently associated with MRD in both the discovery and replication cohorts, we tested the cytotoxicity of NAMPT inhibitors in a panel of 7 B-ALL and 3 T-ALL cell lines. FK866 was the most potent, with IC_{50} values in the low nanomolar range in 8 cell lines. STF 118804 and GPP 78 were effective in most cell lines at doses of 50 nM and 500 nM, respectively (Fig. 4A and B). In general, each cell line showed a consistent degree of sensitivity across all three NAMPT inhibitors, with two B-ALL cell lines demonstrating high sensitivity (RS4;11 and SUP-B15), two B-ALL demonstrating moderate sensitivity (Reh and JM1); and two T-ALL cell lines demonstrating reduced sensitivity (CCRF-CEM and HSB-2). We additionally investigated the cytotoxicity of metformin in each cell line and observed no effect on viability at concentrations up to 500 µM (Figure S3).

Next, we tested our hypothesis that the cytotoxic effects of NAMPT inhibitors are mediated through specific on-target effects on NAD+ availability, by pre-treating two B-ALL cell lines with NAD+ prior to treatment with either NAMPT inhibitor or conventional chemotherapy. As expected, NAD+ supplementation completely prevented NAMPT inhibitor-mediated apoptosis but had no effect on doxorubicin- or etoposide-mediated apoptosis, supporting that the cytotoxic effects of NAMPT inhibitors specifically result from inhibition of NAD+ generation (Fig. 4C).

We also tested the three NAMPT inhibitors in 5 B-ALL patient samples, following expansion in xenografts. FK866 and STF 118804 demonstrated potent cytotoxicity in each of the 5 ALL samples and GPP 78 was slightly less potent. In comparison, doxorubicin had a wider range of IC_{50} values (Fig. 5A and B). Similar to effects observed in ALL cell lines, NAD+ fully rescued ALL patient samples 22763, 2003, 1995, and 105127-R from the cytotoxic effects of the

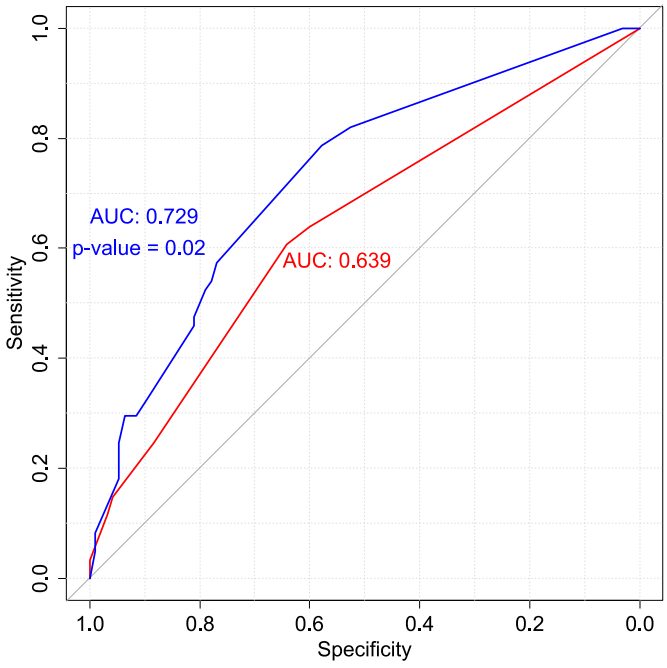

Fig. 3. Receiver operating characteristics curves showing sensitivity, specificity, and area under the curve for predicting end-induction MRD in the clinical and combined models. In red, a clinical model incorporating immunophenotype, NCI risk status, and cytogenetics (favourable/neutral vs. unfavourable); in blue, a model additionally incorporating cluster membership. Models were computed in the combined population of $N = 155$ patients from the discovery and replication cohorts.

NAMPT inhibitor FK866 but not of doxorubicin, as measured by assays of apoptosis (Fig. 5C) and cell viability (Figure S4).

4. Discussion

We conducted global metabolomic profiling of diagnostic bone marrow plasma from children with ALL and identified alterations in central carbon and amino acid metabolism associated with end-induction MRD. MRD-positive samples were characterized by decreased glucose abundances but increased abundances of other metabolites annotating to glycolysis, the pentose phosphate pathway, and the TCA cycle. Importantly, this association did not appear to depend on ALL immunophenotype. The addition of metabolomic data to clinical risk factors improved prediction of end-induction MRD, as measured by AUC. To assess potential clinical applications of these findings, we tested three NAMPT inhibitors in 10 ALL cell lines and five ALL patient samples and found that they exerted potent in vitro cytotoxicity. Additional experiments with two of these samples and two additional samples revealed FK866 functions through an NAD+-dependent mechanism. These results highlight the potential application of metabolomic profiling for risk prediction and targeted therapy in ALL. Specifically, subsets of patients presenting with increased abundances of TCA and pentose phosphate pathway intermediates may be at risk of poor response to induction chemotherapy. Importantly, the increased odds of MRD positivity remained after adjustment for established clinical risk factors, including immunophenotype, NCI risk group, and cytogenetics, suggesting that metabolomic profiling demonstrates independent prognostic value.

To assess the effect of blocking metabolic pathways most associated with MRD, specifically central carbon metabolism, we first

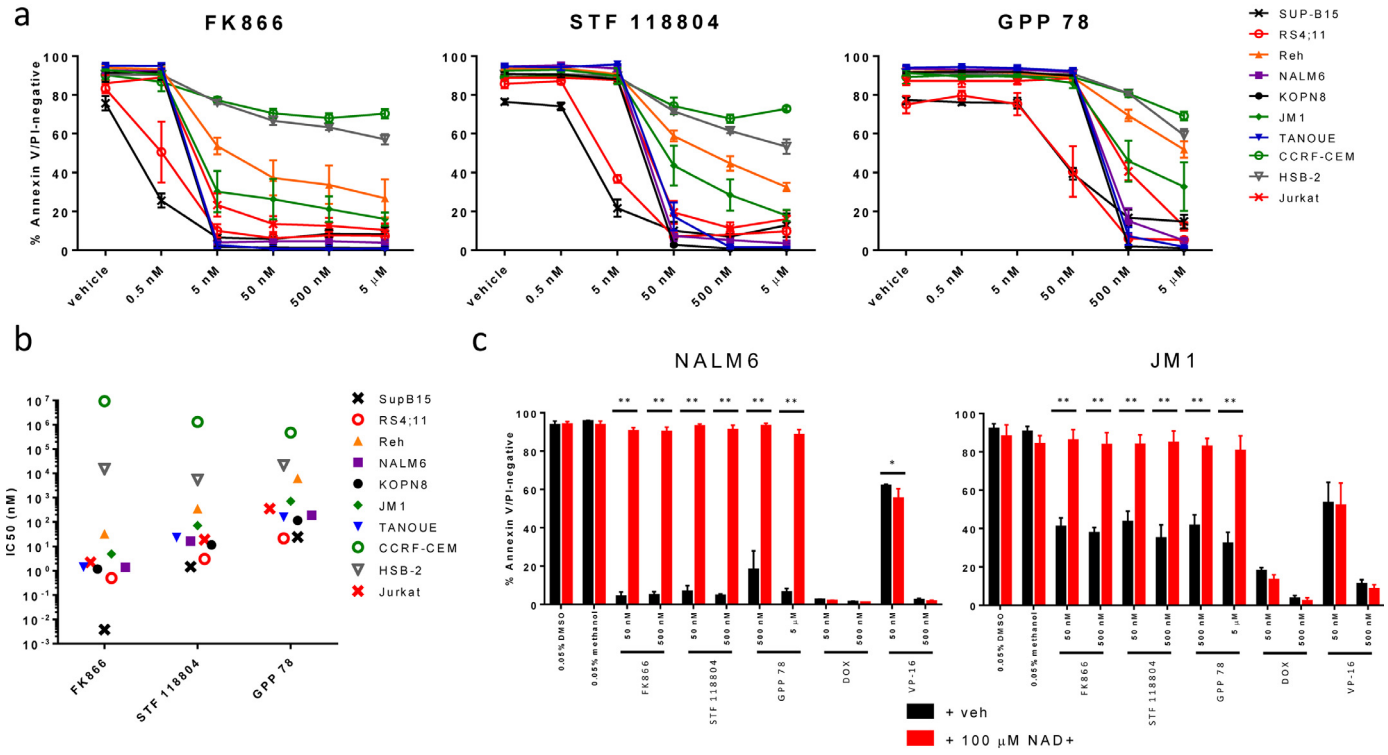

Fig. 4. NAMPT inhibitors demonstrate potent in vitro cytotoxicity in ALL cell lines through NAD+ depletion. (a) Mean percentage (plus or minus standard deviation) of viable cells for 7 B-ALL and 3 T-ALL cell lines incubated for 96 h with each of three NAMPT inhibitors. (b) IC_{50}s (nM) as calculated from data shown in (a). FK866 was the most cytotoxic in the 8 cell lines sensitive to NAMPT inhibition, followed by STF 118804 and GPP 78. T-ALL cell lines CCRF-CEM and HSB-2 were most resistant to each NAMPT inhibitor. (c) Mean percentage (plus or minus standard deviation) of viable cells in the NALM6 (left) and JM1 (right) cell lines when pre-treated with water or 100 μM NAD+, and then incubated for 96 h with indicated agents. NAD+ supplementation prevented apoptosis for all tested doses of NAMPT inhibitors, but not for doxorubicin (DOX) or etoposide (VP-16). Results represent the average of at least four biological replicates across two independent experiments. Differences between groups were calculated with two-way ANOVA and Sidak's multiple comparisons test ($^{*}p < 0{\cdot}05$, $^{**}p < 0{\cdot}0001$).

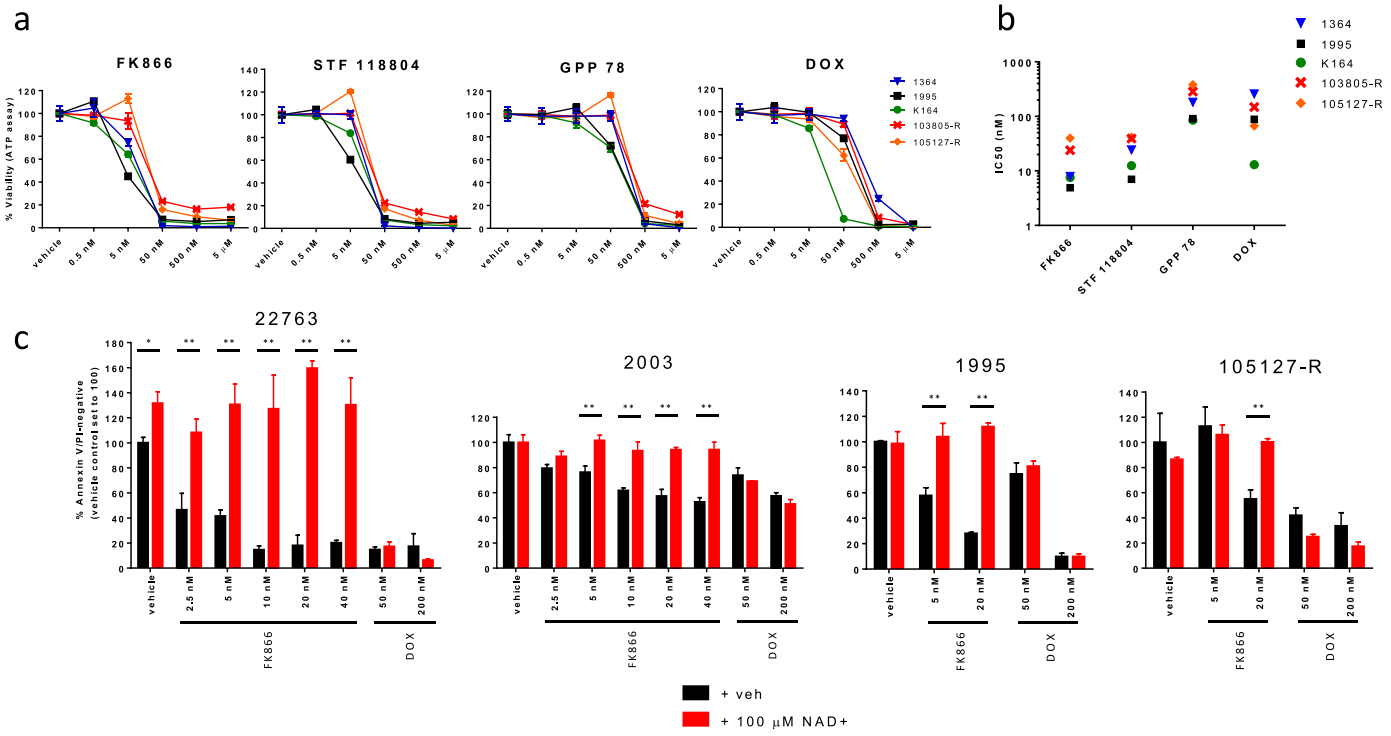

Fig. 5. NAMPT inhibitors demonstrate potent in vitro cytotoxicity in cells from ALL patient-derived xenografts through NAD+ depletion. (a) Viability curves. Samples were incubated for 48 h with each of three NAMPT inhibitors or doxorubicin (DOX), then analysed for viability by ATP assay. Each data point represents the mean and standard deviation of three technical replicates. (b) Summary of IC_{50} values. FK866 demonstrated the lowest IC_{50} in all five samples. Effects of NAD pre-treatment on (c) apoptosis. Patient samples 22763, 2003, 1995, or 105127-R were pre-treated with water or 100 μM NAD+ for one hour, then incubated with FK866 or DOX for 72 h for Annexin V/PI analysis. NAD+ completely prevented increases in mean (plus or minus standard deviation) apoptosis in FK866- but not DOX-treated patient samples. Experiments were performed with triplicate wells. Differences between groups were calculated with two-way ANOVA and Side's multiple comparisons test ($^{*}p < 0{\cdot}05$, $^{**}p < 0{\cdot}001$).

treated cells with metformin. Doses of metformin up to 500 μM had little to no effect on the viability of each of the 7 B-ALL and 3 T-ALL cell lines tested (Figure S3). We then treated B-ALL and T-ALL cell lines and patient samples with inhibitors of NAMPT, which produces NAD+ necessary for the glyceraldehyde 3-phosphate dehydrogenase step in glycolysis. The NAMPT inhibitor FK866 has also been shown to reduce levels of fumarate and malate, 2 of the 3 metabolites independently associated with MRD in both our discovery and replication cohorts [27]. FK866 demonstrated the lowest IC_{50} values among the three NAMPT inhibitors as well as doxorubicin for each of the five ALL patient samples tested. We confirmed that these inhibitors function specifically via reducing available NAD+, as NAD+ supplementation prevented the cytotoxic effects of NAMPT inhibitors but not of other chemotherapeutic agents in cell lines and patient samples. Previous preclinical studies have shown promising activity of NAMPT inhibitors in hematologic malignancies: FK866 in mice xenografted with a Burkitt lymphoma cell line, STF 118804 in B-ALL cells and in mice xenografted with an AML cell line, and KPT-9274 in mice xenografted with a B-ALL patient sample [29–31]. A Phase 1 trial of FK866 demonstrated that the drug was well-tolerated and resulted in 7·5–20·6 nM steady-state plasma concentrations [32], a dose range which demonstrated efficacy in patient samples in our study. Since these compounds affect a general metabolic pathway important in all cells, some studies have included niacin co-administration to rescue normal cells from toxicity. Niacin rescue is most effective if the tumour cells are negative for NAPRT1, which mediates its protective effect. Further studies are needed to determine optimal dosing, NAPRT1 expression profile and other predictors of sensitivity in ALL, and potential synergy of combination regimens [[31],[33]].

Bai et al. performed metabolomic profiling of serum from healthy controls and two groups of ALL patients: those with active disease and those in remission [19]. ALL patients were distinguishable from controls, principally on the basis of glycerophospholipid and fatty acid abundances. The authors hypothesized that these dysregulations reflected increased cell proliferation in ALL. Musharraf et al. were able to differentiate ALL patients from healthy controls as well as from acute myeloid leukaemia and aplastic anaemia patients, and similarly found that lipid metabolites were altered in ALL serum [18]. We detected a number of associations between lipids and MRD in the discovery partition, though none were subsequently replicated. Although these studies provide evidence that metabolite abundances may distinguish ALL patients from healthy controls, ours is the first to demonstrate potential clinical significance of metabolic perturbations.

Key strengths of this study include the use of a two-stage discovery and validation approach for metabolite and pathway discovery, and the functionalization of these results through follow-on experiments. These experiments indicate that NAMPT inhibitors, which target the identified metabolic pathway of central carbon metabolism, exert cytotoxic effects in vitro in ALL cell lines and xenograft-expanded patient samples. This study is the first to test multiple NAMPT inhibitors in an extended panel of ALL cell lines and patient samples, and to demonstrate the dependence of that FK866 cytotoxicity in B-ALL patient samples on NAD+ depletion. These experiments support the plausibility of altered central carbon metabolism as an independent prognostic biomarker and demonstrate that metabolomics may be useful in identifying druggable metabolic alterations in ALL. Importantly, since these samples were collected at diagnosis, this approach could be applied to support early introduction of novel agents.

Table 2
Demographic and clinical characteristics of the study sample according to cluster.

	Cluster 1 ($N = 97$)	Cluster 2 ($N = 58$)	p[a]
Sex, *N*(%)			0.68
Male	57 (58.8)	36 (62.1)	
Female	40 (41.2)	22 (37.9)	
Age [years], median (IQR)	6.5 (8.3)	6.2 (6.5)	
Race-ethnicity, *N*(%)			0.55
NHW	31 (32.0)	14 (24.1)	
Hispanic	57 (58.8)	39 (67.2)	
Other non-Hispanic	9 (9.3)	5 (8.6)	
BMI category[b], *N*(%)			0.90
Normal weight	70 (73.7)	40 (72.7)	
Overweight or obese	25 (26.3)	15 (27.3)	
NCI risk status[c], *N*(%)			0.14
Standard risk	60 (61.9)	28 (48.3)	
High risk	37 (38.1)	30 (51.7)	
Immunophenotype, *N*(%)			0.33
B-lineage	91 (93.8)	51 (87.9)	
T-lineage	7 (12.1)	6 (6.2)	
Cytogenetics[d], *N*(%)			0.20
Favorable or neutral	87 (89.7)	47 (81.0)	
Unfavorable	10 (10.3)	11 (19.0)	
MRD status, *N*(%)			0.001
Negative	70 (72.2)	25 (43.1)	
Positive	27 (27.8)	33 (56.9)	
Early relapse[e], *N*(%)	24 (26.1)	14 (25.5)	0.93

Abbreviations: NHW, non-Hispanic white; BMI, body mass index. MRD, minimal residual disease.

[a] All p-values for categorical values from χ^2 test. p-value for age at diagnosis from Kruskal–Wallis test.

[b] Overweight defined as age- and sex-adjusted BMI ≥85th percentile. Obese defined as age- and sex-adjusted BMI ≥95th percentile. Not computed for children <2 years of age.

[c] High risk defined as presenting white blood cell count >50,000 cells/μL and/or age at diagnosis ≥10 years.

[d] Unfavorable cytogenetics defined as presence of *BCR-ABL1, KMT2A* rearrangement, hypodiploidy (<44 chromosomes), or iAMP21 at diagnosis.

[e] Evaluable in 92 patients in Cluster 1 and 55 patients in Cluster 2.

This study has certain limitations. First, the study included only diagnostic samples. Pre-treatment samples provide an important snapshot of biological features that are important in early treatment response. Future studies of longitudinal samples may provide additional insights into prognostically and therapeutically significant metabolic changes throughout the course of ALL therapy. Since relapse is highly multifactorial, involving both initial disease characteristics, pharmacogenomics, adherence, and other factors, future studies with larger sample size, long-term follow-up, and inclusion of longitudinal samples will be required to fully evaluate the role of metabolomics in prediction of ALL relapse. Although we did not measure malate and fumarate concentrations in treated cells, several investigations have established that NAMPT inhibition results in decreased concentrations of these metabolites [26–28]. Furthermore, our data demonstrating that NAD+ pretreatment abrogates the cytotoxic effects of NAMPT inhibition are concordant with a report from Oakey et al., who showed that NAMPT inhibitor-mediated decreases in malate were attenuated by treatment with nicotinamide riboside [28]. These data suggest that NAMPT inhibitors exert their cytotoxic effects through on-target effects on central carbon metabolism.

In conclusion, we have demonstrated that metabolomic profiling of diagnostic bone marrow plasma provides insights into biological pathways associated with early treatment response in paediatric ALL and may improve risk prediction and identify targetable metabolic vulnerabilities. Specifically, altered central carbon and amino acid metabolism were associated with MRD positivity independent of clinical risk factors, and in vitro data show that NAMPT inhibitors targeting central carbon metabolism reduce viability of ALL cells. While these findings should be independently validated, they demonstrate the potential utility of metabolomics for risk stratification and precision medicine in paediatric ALL. The translational potential of these findings may be expanded by future studies incorporating longitudinal sample collection, and validation in peripheral blood, which could permit rapid, minimally invasive sample collection to support clinical decision-making.

Funding sources

This work was supported by Baylor College of Medicine Department of Paediatrics (Pediatric Pilot Award to PJL), the Cancer Prevention and Research Institute of Texas (CPRIT RP160097 to Margaret R Spitz), the American Society of Hematology (Scholar Award, to JJJ), the Lynch family (to KRR and PJL), the National Cancer Institute at the National Institutes of Health (K07 CA218362 to ALB), and a Consortium Grant by St. Baldrick's Foundation with generous support from the Micaela's Army Foundation (to PJL and KRR). The study sponsors had no role in the study design; in the collection, analysis, and interpretation of data; in the writing of the report; or in the decision to submit for publication.

Author contributions

Contribution: MES, KRR and PJL conceptualized and supervised the research. KRR, PJL and JMS performed project administration, including participant identification and clinical data abstraction. JMS and JJJ developed the methodology and performed formal analysis and visualization. JMS, JJJ and ALB performed data curation. JMS and JJJ wrote the original draft of the paper; all authors participated in review and editing. Dr. Schraw had full access to the data, and had final responsibility for the decision to submit for publication.

Declaration of Competing Interest

The authors have no conflicts of interest to declare.

Acknowledgements

The authors would like to thank the Cytometry and Cell Sorting Core at Baylor College of Medicine with funding from the United States National Institutes of Health (CA125123, and RR024574) and the expert assistance of Joel M Sederstrom. The authors would like to thank Katarzyna Broniowska (Metabolon) for her technical assistance.

Supplementary materials

Supplementary material associated with this article can be found, in the online version, at doi:10.1016/j.ebiom.2019.09.033.

References

[1] Tai EW, Ward KC, Bonaventure A, Siegel DA, Coleman MP. Survival among children diagnosed with acute lymphoblastic leukemia in the United States, by race and age, 2001 to 2009: findings from the CONCORD-2 study. Cancer 2017;123(Suppl 24):5178–89.
[2] Hunger SP, Mullighan CG. Acute lymphoblastic leukemia in children. N Engl J Med 2015;373(16):1541–52.
[3] Roberts KG, Pei D, Campana D, Payne-Turner D, Li Y, Cheng C, et al. Outcomes of children with BCR-ABL1-like acute lymphoblastic leukemia treated with risk-directed therapy based on the levels of minimal residual disease. J Clin Oncol 2014;32(27):3012–20.
[4] Stanulla M, Dagdan E, Zaliova M, Moricke A, Palmi C, Cazzaniga G, et al. IKZF1(plus) defines a new minimal residual disease-dependent very-poor prognostic profile in pediatric B-Cell precursor acute lymphoblastic leukemia. J Clin Oncol 2018 Jco2017743617.

[5] Pui CH, Pei D, Raimondi SC, Coustan-Smith E, Jeha S, Cheng C, et al. Clinical impact of minimal residual disease in children with different subtypes of acute lymphoblastic leukemia treated with response-adapted therapy. Leukemia 2017;31(2):333–9.
[6] O'Connor D, Enshaei A, Bartram J, Hancock J, Harrison CJ, Hough R, et al. Genotype-Specific minimal residual disease interpretation improves stratification in pediatric acute lymphoblastic leukemia. J Clin Oncol 2018;36(1):34–43.
[7] Borssen M, Nordlund J, Haider Z, Landfors M, Larsson P, Kanerva J, et al. DNA methylation holds prognostic information in relapsed precursor B-cell acute lymphoblastic leukemia. Clin Epigenetics 2018;10:31.
[8] Borowitz MJ, Devidas M, Hunger SP, Bowman WP, Carroll AJ, Carroll WL, et al. Clinical significance of minimal residual disease in childhood acute lymphoblastic leukemia and its relationship to other prognostic factors: a children's oncology group study. Blood 2008;111(12):5477–85.
[9] Conter V, Bartram CR, Valsecchi MG, Schrauder A, Panzer-Grumayer R, Moricke A, et al. Molecular response to treatment redefines all prognostic factors in children and adolescents with B-cell precursor acute lymphoblastic leukemia: results in 3184 patients of the AIEOP-BFM ALL 2000 study. Blood 2010;115(16):3206–14.
[10] Matloub Y, Bostrom BC, Hunger SP, Stork LC, Angiolillo A, Sather H, et al. Escalating intravenous methotrexate improves event-free survival in children with standard-risk acute lymphoblastic leukemia: a report from the children's oncology group. Blood 2011;118(2):243–51.
[11] Larsen EC, Devidas M, Chen S, Salzer WL, Raetz EA, Loh ML, et al. Dexamethasone and high-dose methotrexate improve outcome for children and young adults with high-risk B-Acute lymphoblastic leukemia: a report from children's oncology group study AALL0232. J Clin Oncol 2016;34(20):2380–8.
[12] Vrooman LM, Stevenson KE, Supko JG, O'Brien J, Dahlberg SE, Asselin BL, et al. Postinduction dexamethasone and individualized dosing of *Escherichia coli* L-asparaginase each improve outcome of children and adolescents with newly diagnosed acute lymphoblastic leukemia: results from a randomized study–Dana-Farber cancer institute all consortium protocol 00-01. J Clin Oncol 2013;31(9):1202–10.
[13] Burke MJ, Salzer WL, Devidas M, Dai Y, Gore L, Hilden JM, et al. Replacing cyclophosphamide/cytarabine/mercaptopurine with cyclophosphamide/etoposide during consolidation/delayed intensification does not improve outcome for pediatric B-cell acute lymphoblastic leukemia: a report from the COG. Haematologica 2019;104(5):986–92.
[14] Salzer WL, Burke MJ, Devidas M, Chen S, Gore L, Larsen EC, et al. Toxicity associated with intensive postinduction therapy incorporating clofarabine in the very high-risk stratum of patients with newly diagnosed high-risk B–lymphoblastic leukemia: a report from the children's oncology group study AALL1131. Cancer 2018;124(6):1150–9.
[15] McNeer JL, Devidas M, Dai Y, Carroll AJ, Heerema NA, Gastier-Foster JM, et al. Hematopoietic stem-cell transplantation does not improve the poor outcome of children with hypodiploid acute lymphoblastic leukemia: a report from children's oncology group. J Clin Oncol 2019;37(10):780–9.
[16] Clish CB. Metabolomics: an emerging but powerful tool for precision medicine. Cold Spring Harb Mol Case Stud 2015;1(1):a000588.
[17] Tiziani S, Kang Y, Harjanto R, Axelrod J, Piermarocchi C, Roberts W, et al. Metabolomics of the tumor microenvironment in pediatric acute lymphoblastic leukemia. PLoS ONE 2013;8(12):e82859.
[18] Musharraf SG, Siddiqui AJ, Shamsi T, Naz A. SERUM metabolomics of acute lymphoblastic leukaemia and acute myeloid leukaemia for probing biomarker molecules. Hematol Oncol 2016.
[19] Bai Y, Zhang H, Sun X, Sun C, Ren L. Biomarker identification and pathway analysis by serum metabolomics of childhood acute lymphoblastic leukemia. Clin Chim Acta 2014;436:207–16.
[20] Dhakshinamoorthy S, Dinh NT, Skolnick J, Styczynski MP. Metabolomics identifies the intersection of phosphoethanolamine with menaquinone-triggered apoptosis in an in vitro model of leukemia. Mol Biosyst 2015;11(9):2406–16.
[21] Bannur Z, Teh LK, Hennesy T, Rosli WR, Mohamad N, Nasir A, et al. The differential metabolite profiles of acute lymphoblastic leukaemic patients treated with 6-mercaptopurine using untargeted metabolomics approach. Clin Biochem 2014;47(6):427–31.
[22] Cheung YT, Khan RB, Liu W, Brinkman TM, Edelmann MN, Reddick WE, et al. Association of cerebrospinal fluid biomarkers of central nervous system injury with neurocognitive and brain imaging outcomes in children receiving chemotherapy for acute lymphoblastic leukemia. JAMA Oncol 2018;4(7):e180089.
[23] Reikvam H, Hatfield K, Bruserud O. The pretransplant systemic metabolic profile reflects a risk of acute graft versus host disease after allogeneic stem cell transplantation. Metab: Official J Metab Soc 2016;12(1):12.
[24] Huss M, Holme P. Currency and commodity metabolites: their identification and relation to the modularity of metabolic networks. IET Syst Biol 2007;1(5):280–5.
[25] Bergaggio E, Riganti C, Garaffo G, Vitale N, Mereu E, Bandini C, et al. IDH2 inhibition enhances proteasome inhibitor responsiveness in hematological malignancies. Blood 2019;133(2):156–67.
[26] Tolstikov V, Nikolayev A, Dong S, Zhao G, Kuo MS. Metabolomics analysis of metabolic effects of nicotinamide phosphoribosyltransferase (NAMPT) inhibition on human cancer cells. PLoS ONE 2014;9(12):e114019.
[27] Tan B, Young DA, Lu ZH, Wang T, Meier TI, Shepard RL, et al. Pharmacological inhibition of nicotinamide phosphoribosyltransferase (NAMPT), an enzyme essential for NAD+ biosynthesis, in human cancer cells: metabolic basis and potential clinical implications. J Biol Chem 2013;288(5):3500–11.
[28] Oakey LA, Fletcher RS, Elhassan YS, Cartwright DM, Doig CL, Garten A, et al. Metabolic tracing reveals novel adaptations to skeletal muscle cell energy production pathways in response to NAD (+) depletion. Wellcome Open Res 2018;3:147.
[29] Nahimana A, Aubry D, Breton CS, Majjigapu SR, Sordat B, Vogel P, et al. The anti-lymphoma activity of APO866, an inhibitor of nicotinamide adenine dinucleotide biosynthesis, is potentialized when used in combination with anti-CD20 antibody. Leuk Lymphoma 2014;55(9):2141–50.
[30] Matheny CJ, Wei MC, Bassik MC, Donnelly AJ, Kampmann M, Iwasaki M, et al. Next-generation NAMPT inhibitors identified by sequential high-throughput phenotypic chemical and functional genomic screens. Chem Biol 2013;20(11):1352–63.
[31] Takao S, Chien W, Madan V, Lin DC, Ding LW, Sun QY, et al. Targeting the vulnerability to NAD(+) depletion in B-cell acute lymphoblastic leukemia. Leukemia 2018;32(3):616–25.
[32] Holen K, Saltz LB, Hollywood E, Burk K, Hanauske AR. The pharmacokinetics, toxicities, and biologic effects of FK866, a nicotinamide adenine dinucleotide biosynthesis inhibitor. Invest New Drugs 2008;26(1):45–51.
[33] Roulston A, Shore GC. New strategies to maximize therapeutic opportunities for NAMPT inhibitors in oncology. Mol Cell Oncol 2016;3(1):e1052180.